Dégivrage de gouttes sur un plan incliné

Melting droplet on an inclined plane

Sergio Peralta Ventocilla[1], **Julien Sebilleau**[1], **Guillaume Castanet**[2], **Dominique Legendre**[1], **Mehdi Stiti**[1*]

[1] IMFT, Université de Toulouse, CNRS, 3100, Toulouse, France
[2] LEMTA, Université de Lorraine, CNRS, 5400, Nancy, France
*(Corresponding author: mehdi.stiti@imft.fr)

Résumé - La dynamique de fusion et de glissement d'une goutte d'eau initialement gelée sur un substrat hydrophobe incliné est étudiée expérimentalement. Trois régimes — statique, inertie modérée et forte inertie — sont identifiés à l'aide d'un nombre de Bond modifié combinant les effets gravitaires et capillaires. Le dégivrage par chauffage par le bas favorise le décollement en générant une couche liquide interfaciale. Le mouvement de la goutte accélère la fusion, tandis que l'épaisseur critique de liquide augmente avec le diamètre de contact et dépend faiblement de l'inclinaison.

Abstract - The melting and sliding dynamics of an initially frozen water droplet on an inclined hydrophobic substrate are investigated experimentally. Three regimes—static, moderate inertia and high inertia—are identified using a modified Bond number combining gravitational and capillary effects. Bottom-up melting promotes depinning by forming an interfacial liquid layer. Droplet motion is shown to accelerate melting, while the critical liquid layer thickness increases with contact diameter and weakly depends on inclination.

Nomenclature

t	time, s
T	temperature, C
V	Volume, L
$\vec{k}$	unit vector
Bo	Bond number
h	thickness, m

Greek symbols

β	angle,
ρ	density, kg/m^3
σ	surface tension, N/m

1. Introduction

Droplet freezing and melting are ubiquitous phenomena that play a critical role in natural and industrial applications. Understanding these processes is essential to predict and mitigate ice accretion on aircraft [6], reduce operational risks in wind energy production [13], and ensure the reliability of overhead power lines in cold climates. Beyond icing-related issues, droplet solidification and melting influence additive manufacturing, where phase-change dynamics affect material properties and thermal energy storage in phase-change materials [1]. These applications motivate systematic experimental and theoretical investigations to characterize droplet freezing and melting and improve predictive models. From a fundamental viewpoint, droplet freezing and melting on a substrate can be considered as containerless phase-change configurations [2], involving heat transfer, phase change, moving phase boundaries, and surface tension effects [8]. Despite their relevance, most studies focus on freezing, while melting dynamics

https://doi.org/10.25855/SFT2026-058

remain comparatively unexplored [12]. Melting may appear as the reverse of freezing, yet important differences arise. Zhang et al. [15] showed that water droplet melting occurs near 0.5 °C, with minimal superheating, whereas freezing requires significant supercooling. Characteristic time scales differ due to the contrast in thermal diffusivity between ice and liquid water [5]. Internal flow dynamics also differ: convective flows are more pronounced during melting, primarily driven by thermocapillary effects, even for small temperature differences and thin liquid layers [9]. Marangoni convection has been reported during melting on superhydrophobic substrates [14]. Recent studies highlight the combined influence of thermocapillary and thermogravitational effects on melting [3]. Cui et al. [4] proposed a dewetting strategy using freezing–melting cycles, showing that melting can induce droplet depinning on mechanically fragile superhydrophobic surfaces. Strong thermocapillary flows may also modify melting modes: Lei et al. [11] showed that intense Marangoni flows push the solid phase into the droplet, establishing full ice–liquid contact and reducing melting time. In many practical situations, droplet freezing occurs on inclined surfaces, introducing a gravitational component. Freezing on inclined subcooled substrates has been studied experimentally and numerically [7], but melting of iced droplets under similar conditions remains poorly explored. Jin et al. [10] examined droplet impact, freezing, and melting on inclined cold surfaces, yet droplets remained stationary during melting, and sliding dynamics were not addressed. To date, no systematic study has examined the coupled melting and sliding of a frozen droplet on a heated inclined substrate. This work presents an experimental investigation of an initially frozen water droplet deposited on a hydrophobic inclined surface and heated from below. The study focuses on de-icing dynamics, including the formation of the interfacial liquid layer during melting and the onset of droplet sliding. Key aspects include the influence of droplet volume and substrate inclination on depinning, the interplay between capillary forces and gravity, and the coupling between sliding motion and melting kinetics. These observations aim to provide a foundation for predictive modeling of droplet sliding during phase change, relevant for icing mitigation and heat-transfer applications.

2. Experimental setup

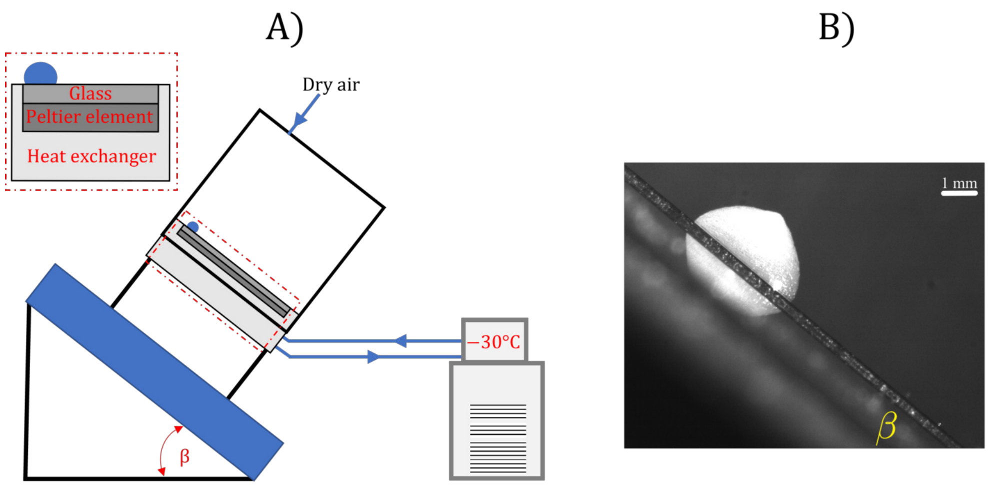

Figure 1: A) Experimental setup for studying the de-icing of a single water droplet on an inclined, thermally controlled substrate. B) Side-view image of a solidified droplet on the inclined surface prior to melting.

The experimental setup is designed to investigate the de-icing dynamics of a single water droplet as a function of the inclination angle of the substrate. The core element of the setup consists of a flat glass plate mounted on a controllable inclination system. The glass substrate is chemically treated using a silanization process in order to obtain a hydrophobic surface, thereby limiting contact line pinning and ensuring reproducible wetting conditions. The treated glass plate is placed directly on top of a Peltier thermoelectric module, which enables both precise temperature regulation and rapid heating of the substrate. The surface temperature of the glass plate is monitored and regulated using an electrical control system coupled to the Peltier module. This configuration allows controlled transitions between freezing and melting regimes, which are essential for studying the de-icing process under well-defined thermal conditions. To ensure efficient heat removal and to reach low substrate temperatures, the Peltier module is coupled on its cold side to a plate heat exchanger. This heat exchanger is connected to a Julabo refrigerated heat exchanger, capable of cooling the system down to -40°C. The combined use of the Peltier module and the external cooling loop provides a wide and well-controlled temperature range, as well as fast thermal response times. The entire assembly is housed inside a closed environmental chamber. Dry air with a dew point of -40°C is continuously injected into the chamber to suppress condensation and frost formation on the substrate and surrounding components. This controlled atmosphere ensures stable and repeatable experimental conditions during both freezing and melting stages.

The objective of the optical measurements is to investigate the de-icing dynamics, which encompasses not only the sliding motion of the droplet along the inclined surface, but also the conditions required to initiate sliding. In particular, special attention is paid to the minimum liquid layer thickness necessary to enable droplet motion. To characterize the droplet shape evolution and the ice–liquid interface during the de-icing process, optical measurements are performed using a side-view shadowgraphy configuration. In order to enhance the contrast between the solid ice phase, which strongly reflects light, and the liquid phase, the droplet is illuminated along the flow direction, providing a well-defined intensity gradient suitable for accurate interface detection. Two different optical objectives are used depending on the measurement objective. A low-magnification objective (80 µm/pixels) is employed to capture the global sliding dynamics of the droplet along the inclined surface, which has a characteristic length of 5 cm. In contrast, a higher-magnification objective (7 µm/pixels) is used to zoom in on the droplet, enabling a detailed investigation of the solidification and melting front evolution within the droplet. An example of the visualisation of the droplet using the high magnification zoom is shown in Fig.1B.

3. Melting-induced sliding on inclined surfaces: critical angle and regimes

In this section, the focus is placed on determining the minimum inclination angle required to trigger droplet sliding during the de-icing process. The experimental protocol is designed accordingly. A water droplet of volume V_0 is first deposited and frozen on the glass substrate maintained at an inclination angle of $\beta = 0°$. Once the droplet is fully solidified, the experimental assembly is tilted to a given inclination angle, and de-icing is initiated by imposing a constant heating rate of 2.25°C/s delivered by the Peltier module. This procedure allows the coupled effects of melting, gravity, and thermal inertia to be systematically investigated and enables the identification of the critical conditions leading to droplet motion. Additionally, for the typical water droplet sizes considered here ($\mathcal{O}(10^{-3})$ m), surface tension forces are also significant in the droplet kinematics.Therefore, the dimensionless Bond number is employed to characterize the present droplet dynamics, as it naturally combines gravitational and capillary

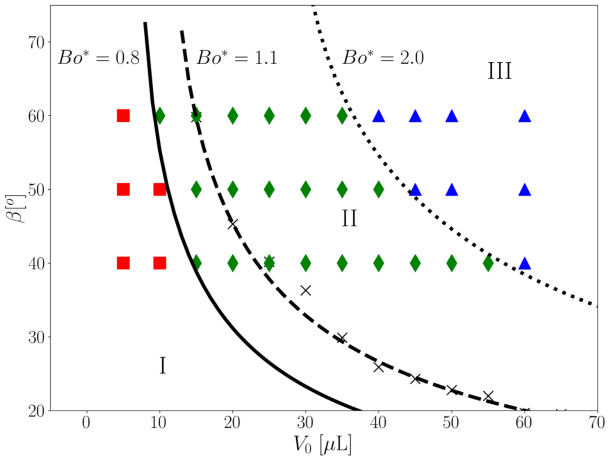

Figure 2: Evolution of the critical inclination angle for the onset of droplet sliding as a function of the initial droplet volume. Experimental conditions are classified into three regimes: static, moderate-inertia, and high-inertia.

effects. The Bond number is defined as:

$$Bo^* = \frac{D_{eq}^2\, g\, \rho_l\, \sin\beta}{\sigma}, \tag{1}$$

where $D_{eq} = (6V_0/\pi)^{1/3}$ is the equivalent droplet diameter based on the initial droplet volume V_0 . In the experimental images obtained in this study, three distinct sliding patterns are identified. Each pattern corresponds to a specific region in Fig.2, which are indicated by filled markers (■, ♦, and ▲). For clarity, these regions are also labeled (I), (II), and (III) in Fig.2. In region (I), the droplet remains stationary and does not slide along the substrate during the de-icing process, even as melting progresses, until the iced droplet is fully melted. In region (II), the droplet exhibits a smooth sliding motion characterized by a relatively low velocity. In contrast, region (III) corresponds to a regime in which the droplet slides at significantly higher velocities. Accordingly, the sliding patterns associated with regions (I), (II), and (III) are hereafter referred to as the static, moderate-inertia, and high-inertia regimes, respectively. To provide a physical interpretation of these regimes, contours of the modified Bond number Bo^* are superimposed in Fig.2. In particular, the contours corresponding to $Bo^* = 0.8$ and $Bo^* = 2$ are shown to highlight the transitions between regions (I), (II), and (III). It should be emphasized that these contours do not represent sharp thresholds between the different sliding patterns. Rather, the transitions observed experimentally are gradual, and the Bo^* contours are displayed for reference only. The kinematics of isothermal water droplets sliding on the present glass substrate provide an essential reference framework for interpreting the melting–sliding dynamics investigated in this work. To this end, a systematic analysis of the same configuration in the absence of phase change was performed. The corresponding experimental results are represented by $\times$ markers in Fig.2 and indicate the critical conditions at which isothermal water droplets begin to slide. In addition, the $Bo^* = 1.1$ contour is plotted in Fig.2 as a dashed black line. This contour shows good agreement with the experimentally determined sliding threshold under isothermal conditions, as it corresponds to a regime in which the droplet inertia becomes sufficient to overcome retention forces and initiate motion on the inclined glass substrate. An intermediate region is therefore identified between the $Bo^* = 0.8$ and $Bo^* = 1.1$ contours. In this region, isothermal water droplets remain pinned on the inclined surface, whereas sliding is systematically observed when bottom-up melting is induced. This highlights the crucial role played by the liquid layer generated during de-icing in reducing adhesion and enabling droplet motion.

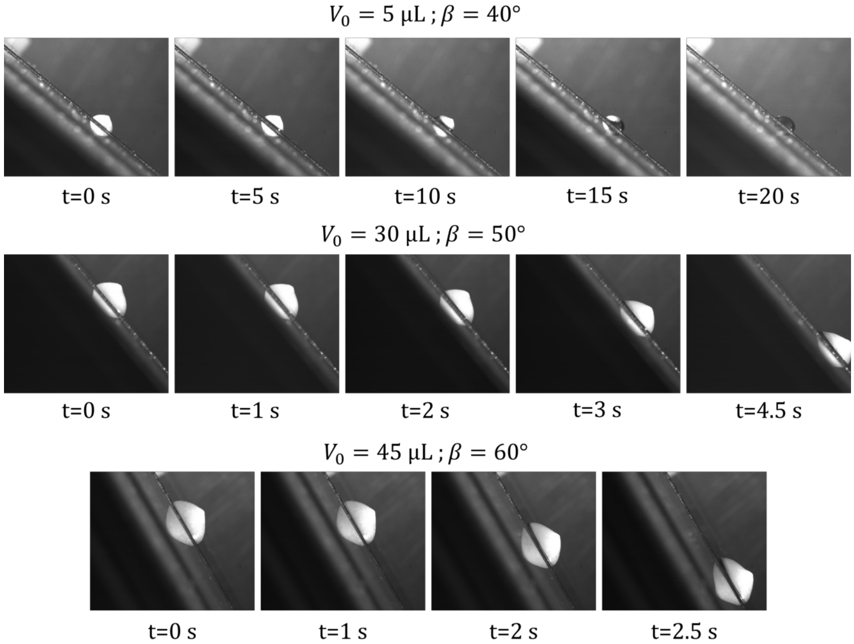

Figure 3: Examples of droplet de-icing dynamics for different initial droplet volumes and substrate inclination angles.

Experimental observations of the melting evolution of droplets with volumes of 5 μL, 30 μL, and 45 μL, for substrate inclination angles of 40), 50°, and 60°, respectively, are presented in Fig.3. In the case of the 5 μL droplet, the droplet remains pinned to the surface throughout the entire melting process, corresponding to the static regime identified in Fig.2. Under these conditions, the gravitational force component parallel to the inclined substrate remains too weak to overcome capillary retention at the contact line. As a result, de-icing occurs entirely at the droplet–substrate interface, and the droplet melts in place without exhibiting any sliding motion. In contrast, increasing the droplet volume leads to qualitatively different sliding dynamics, reflecting a transition from moderate- to high-inertia regimes. Fig.4 presents the temporal evolution of the droplet velocity for three droplet volumes at a fixed inclination angle of 40°. For the intermediate case (30 μL, green markers), the droplet velocity exhibits a two-stage evolution: an initial phase of slow acceleration, followed by a sudden increase in acceleration. This behavior is characteristic of the moderate-inertia regime, in which gravitational forces progressively overcome capillary retention as melting proceeds and the liquid layer at the substrate thickens. By contrast, for larger droplets (45 μL and 60 μL), the velocity increases abruptly immediately after the onset of motion, without the intermediate slow-acceleration phase. These cases correspond to the high-inertia regime, where the droplet weight is sufficiently large to rapidly dominate capillary forces once depinning occurs, leading to a sharp acceleration of the droplet along the inclined surface.

Fig.4 presents the temporal evolution of the ratio between the liquid and solid (ice) surface areas during the melting process. The solid surface is represented as white in Fig.3. This representation provides direct insight into the dynamics of the de-icing front and its coupling with the droplet sliding motion. In this configuration, the influence of the sliding velocity on the melting dynamics can be clearly identified. A marked acceleration of the de-icing process is observed as the droplet sliding velocity increases. Specifically, droplets exhibiting higher sliding velocities

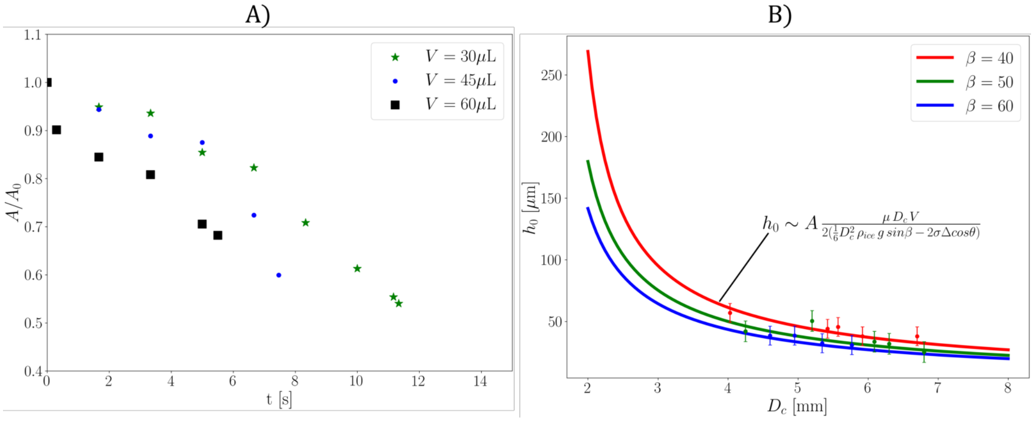

Figure 4: A) Temporal evolution of the ratio between ice-covered and liquid-covered surface areas for different initial droplet diameters at an inclination angle of 30°. B) Evolution of the measured critical liquid-layer thickness as a function of the droplet contact diameter for different substrate inclination angles. Solid lines correspond to fits based on a force balance between the projected droplet weight, capillary retention, and viscous dissipation within the liquid layer.

show a significantly faster increase of the liquid surface fraction, indicating a more rapid retreat of the ice–liquid interface. This behavior highlights the strong coupling between the hydrodynamic motion of the droplet and the phase-change process. This acceleration can be attributed to several concurrent mechanisms. As the droplet slides along the inclined surface, the relative motion enhances heat transfer at the ice–substrate and ice–liquid interfaces by promoting advective transport within the liquid phase. In addition, faster sliding is associated with stronger internal flows, which facilitate heat redistribution inside the droplet and reduce thermal gradients near the melting front. As a result, the melting front advances more rapidly for droplets in the moderate- and high-inertia regimes compared to slowly moving or static droplets. These observations demonstrate that droplet motion does not merely accompany the de-icing process but actively contributes to accelerating it. The results further emphasize the critical role of sliding dynamics in controlling the overall de-icing kinetics, particularly in regimes where inertia dominates capillary resistance.

4. Onset of sliding: critical liquid-layer thickness during de-icing

If we now consider the minimum thickness required for the drop to slide, we can initially assume a gravity-driven flow of a thin water film down an inclined plane, disregarding the effects related to melting. Considering this type of flow, it is possible to show that a minimum thickness of 70 μm is necessary to induce flow. Therefore, in the following, we will only consider the results obtained with the small field of view lens, which provides a resolution of around 7 μm/pixels.

From the side-view images, it is possible to quantify the evolution of the liquid layer thickness at the droplet–substrate interface from which droplet motion is initiated. This thickness corresponds to the minimum liquid layer required to trigger sliding during the de-icing process. Fig.4 presents the evolution of this critical liquid layer thickness as a function of the droplet contact diameter, defined as the diameter of the droplet–substrate contact area measured after solidification and prior to the onset of melting. The measurements are reported for several substrate inclination angles, enabling the combined influence of droplet geometry and inclination on the onset of sliding to be assessed. This representation provides direct insight into the conditions required for droplet depinning during melting and highlights the respective roles of contact area and gravitational forcing in controlling the transition from a pinned to a sliding state. A clear increase in the critical liquid layer thickness required for sliding is observed with increasing droplet–substrate contact area. Larger contact diameters are associated with stronger capillary retention forces, which must be overcome by a thicker interfacial liquid layer before motion can occur. In addition, a weaker but systematic dependence on the inclination angle is observed, with the critical thickness tending to increase as the inclination angle decreases, consistent with the reduction of the gravitational driving force projected along the substrate.

To rationalize these trends, a modelling approach is subsequently introduced based on a balance between the projected weight of the droplet, the capillary retention forces at the contact line, and the viscous dissipation occurring within the liquid layer formed during melting. This viscous dissipation originates from internal flows inside the droplet induced by two coupled mechanisms. First, the de-icing process itself generates liquid motion due to the continuous melting of the ice phase at the droplet–substrate interface. Second, as the solid ice cap melts, it continuously adjusts toward a new equilibrium position, inducing additional internal circulation during droplet motion. These internal flows contribute to energy dissipation within the liquid layer and play a key role in determining the critical conditions required for droplet depinning and subsequent sliding.

In Fig.4 , the scaling law derived from this model is reported together with the experimental data. The proposed scaling successfully captures the main experimental trends, namely the increase of the critical liquid layer thickness with the droplet contact diameter and its comparatively weak dependence on the inclination angle. However, the model does not predict the absolute magnitude of the critical liquid layer thickness. A single multiplicative prefactor, identical for all experimental conditions, is therefore introduced to fit the experimental data. This prefactor can be interpreted as an effective dissipation length scale that is not explicitly resolved in the present formulation. In particular, the simplified description of viscous dissipation does not fully account for localized flow structures near the contact line, within the wedge-shaped interfacial liquid film, or around the partially molten solid cap. The introduction of this empirical dissipation length scale thus highlights the limitations of the current modelling approach and indicates that a more detailed description of the interfacial hydrodynamics and internal flow topology is required to fully capture the melting–sliding dynamics observed experimentally.

5. Conclusion

This work investigated experimentally the melting and sliding dynamics of an initially frozen water droplet on an inclined hydrophobic substrate. The focus was placed on identifying the conditions required for droplet depinning during de-icing and on characterising the resulting sliding regimes. Three distinct behaviours were identified—static, moderate-inertia, and high-inertia—organised by a modified Bond number that captures the balance between gravitational forcing and capillary retention. Comparison with isothermal reference experiments demonstrated that bottom-up melting substantially reduces the sliding threshold, enabling droplet motion in conditions where isothermal droplets remain pinned. This highlights the key role of the interfacial liquid layer formed during de-icing. Velocity measurements revealed clear differences between moderate- and high-inertia regimes, while analysis of the liquid-to-solid surface ratio showed that droplet motion significantly accelerates the melting process through enhanced internal advection and heat transfer. The minimum liquid layer thickness required for sliding was quantified and found to increase with droplet contact diameter and to depend weakly on the inclination angle. A scaling model based on a balance between droplet weight, capillary forces, and viscous dissipation within the liquid layer captures the main experimental trends. However, an empirical prefactor was required to match the absolute values, indicating that additional dissipation mechanisms, not fully resolved in the present model, remain to be incorporated. These results emphasise the strongly coupled thermo-hydrodynamic nature of droplet de-icing and provide a basis for improved predictive models of melting-induced droplet motion on inclined surfaces.

References

[1] I. Ahmad, R. Kumar, U. Ghosh, and A. Bhargav. Consistent description of phase-change processes in substances with density contrast: a finite volume based approach. *International Journal of Thermal Sciences*, 192:108385, 2023.

[2] D. Anderson, M. G. Worster, and S. Davis. The case for a dynamic contact angle in containerless solidification. *Journal of crystal growth*, 163(3):329–338, 1996.

[3] J. Cui, T. Wang, and Z. Che. Melting process of frozen sessile droplets on superhydrophobic surfaces. *Langmuir*, 39(41):14800–14810, 2023.

[4] J. Cui, T. Wang, and Z. Che. Freezing–melting mediated dewetting transition for droplets on superhydrophobic surfaces with condensation. *Langmuir*, 40(28):14685–14696, 2024.

[5] S. H. Davis. *Theory of solidification*. Cambridge University Press, 2001.

[6] R. W. Gent, N. P. Dart, and J. T. Cansdale. Aircraft icing. *Philosophical Transactions of the Royal Society of London. Series A: Mathematical, Physical and Engineering Sciences*, 358(1776): 2873–2911, 2000.

[7] N. X. Ho and T. V. Vu. Solidification of a liquid drop enclosing a bubble on an inclined surface. *European Journal of Mechanics-B/Fluids*, 103:259–268, 2024.

[8] A. Huerre, C. Josserand, and T. Séon. Freezing and capillarity. *Annual Review of Fluid Mechanics*, 57, 2024.

[9] J. Ivall, J.-S. Renault-Crispo, S. Coulombe, and P. Servio. Ice-dependent liquid-phase convective cells during the melting of frozen sessile droplets containing water and multiwall carbon nanotubes. *International Journal of Heat and Mass Transfer*, 101:27–37, 2016.

[10] Z. Jin, D. Sui, and Z. Yang. The impact, freezing, and melting processes of a water droplet on an inclined cold surface. *International journal of heat and mass transfer*, 90:439–453, 2015.

[11] S. Lei, Y. Lee, Y. Li, and J. Shiomi. Enhanced ice melting by strong marangoni convection. *International Journal of Heat and Mass Transfer*, 248:127173, 2025.

[12] S. Lyu, K. Wang, Z. Zhang, A. Pedrono, C. Sun, and D. Legendre. A hybrid vof-ibm method for the simulation of freezing liquid films and freezing drops. *Journal of Computational Physics*, 432: 110160, 2021.

[13] E. Madi, K. Pope, W. Huang, and T. Iqbal. A review of integrating ice detection and mitigation for wind turbine blades. *Renewable and Sustainable Energy Reviews*, 103:269–281, 2019.

[14] L. Wang, Z. Tian, G. Jiang, X. Luo, C. Chen, X. Hu, H. Zhang, and M. Zhong. Spontaneous dewetting transitions of droplets during icing & melting cycle. *Nature communications*, 13(1):378, 2022.

[15] X. Zhang, X. Wu, and J. Min. Freezing and melting of a sessile water droplet on a horizontal cold plate. *Experimental Thermal and Fluid Science*, 88:1–7, 2017.